Dynamical behaviour of the resistive switching in ceramic YBCO/metal interfaces

2011 J. Phys. D: Appl. Phys. 44 345301

(http://iopscience.iop.org/0022-3727/44/34/345301)

IOP PUBLISHING JOURNAL OF PHYSICS D: APPLIED PHYSICS

J. Phys. D: Appl. Phys. **44** (2011) 345301 (4pp) doi:10.1088/0022-3727/44/34/345301

Dynamical behaviour of the resistive switching in ceramic YBCO/metal interfaces

C Acha

Laboratorio de Bajas Temperaturas, Departamento de Física, FCEyN, Universidad de Buenos Aires and IFIBA, CONICET, Pabellón I, Ciudad Universitaria, C1428EHA Buenos Aires, Argentina

E-mail: acha@df.uba.ar

Received 23 March 2011, in final form 14 June 2011
Published 10 August 2011
Online at stacks.iop.org/JPhysD/44/345301

Abstract

Studies related to the dynamics of resistive switching (RS) in ceramic YBCO/metal interfaces were performed. The change in interface resistance during the application of square pulses and its current–voltage (I–V) characteristics were measured. The obtained non-linear current dependence of the differential resistance can be very well reproduced by modelling the electrical behaviour of the interface with simple circuit elements. The RS produces defined changes in the parameters of the circuit model that reveal the particular dynamics of the mechanism beneath the resistance change in complex oxide/metal interfaces.

(Some figures in this article are in colour only in the electronic version)

1. Introduction

In recent years numerous papers have been published on the subject of electric pulse-induced resistive switching (RS) effect observed in many metal–oxide interfaces [1–8]. Technological interest in obtaining new memory devices, such as the resistive RAM device, which consume less energy and can be scaled down to smaller dimensions than the current flash memories [9] is encouraging basic research on the RS effect. One of the objectives is to gain a perfect control on the parameters involved in the change and the stability of the resistive states obtained for these devices.

Most of the studies performed until now have particularly focused on trying to reveal the key parameters that determine the existence of the RS effect [7, 10] (such as the different metal–oxide interfaces or the pulsing protocols) and which are the characteristics of the non-volatile resistance memory state (such as the repeatability and retentivity of the remanent resistance after the pulsing treatment) [11]. It was also established that, for some binary oxide devices [12, 13] and for perovskite oxide devices [14], RS is directly associated with the electromigration of oxygen ions (or vacancies).

Here, attention is focused on the dynamics of the RS. In particular, studies of the I–V characteristics of YBCO ($YBa_2Cu_3O_7$)/(Au or Pt) interfaces are presented in order to understand part of their dynamical behaviour and to reveal additional features of the mechanism beneath the RS effect. These results can be reproduced by considering a simple circuit model to describe the non-linear behaviour of the I–V curves of the interface resistance that, additionally, captures the dynamics and the influence on each particular parameter during the switching process.

2. Experimental

In order to study the switching behaviour of the YBCO/metal interface resistance, four Au or Pt electrodes were sputtered on one of the faces of a YBCO textured ceramic sample. Details of the YBCO synthesis and characteristics of the resistive switching behaviour can be found elsewhere [8, 15]. Here, only the results of the YBCO/Au interfaces are presented as very similar effects were observed for Pt electrodes. The sputtered electrodes have a width of 1 mm and a mean separation between 0.4 and 0.8 mm. They cover the entire width of one of the faces of the YBCO slab ($8 \times 4 \times 0.5\,mm^3$). Finally, silver paint was used carefully to fix copper leads without directly contacting the surface of the sample.

As depicted in figure 1, voltage pulses were applied on electrodes 1 and 2 (arbitrarily defined as + and −, respectively).

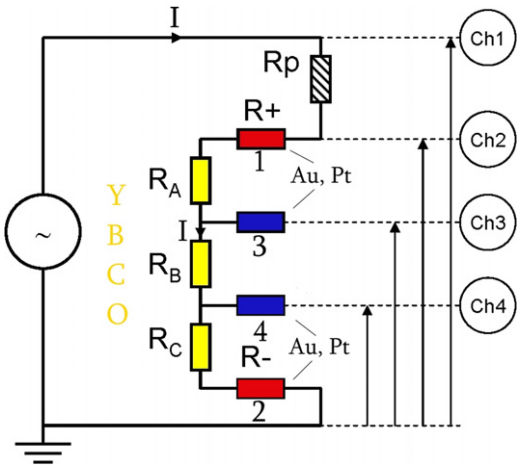

Figure 1. Electric circuit and contact configuration used to study the dynamics of the EPIR switching on YBCO/metal interfaces (Au or Pt). The connections to the oscilloscope channels are also indicated.

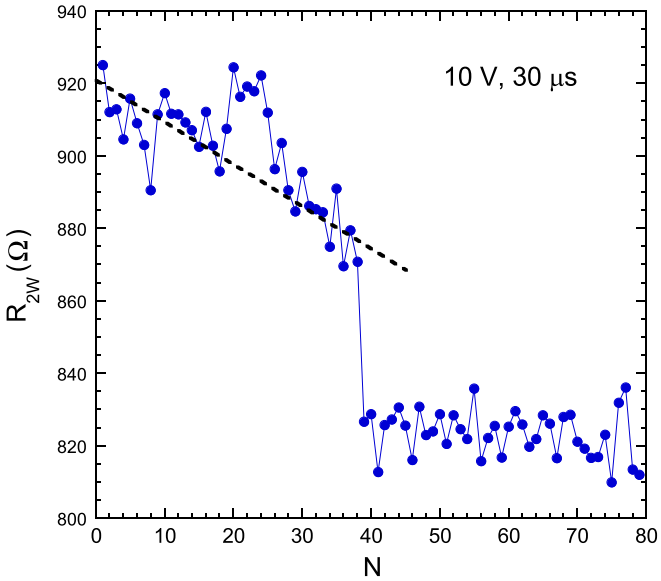

Figure 2. Two terminal resistance (R_{2W}) as a function of the number of square pulses N (of 10 V, 30 μs width). Lines are guides to the eye.

As the four terminal resistance of YBCO is in the 0.1 Ω range ($R_B \simeq 0.1\,\Omega \sim R_A \sim R_C$) [8], the contact resistance can be estimated by measuring the voltage drops between contacts 1–3 ($R^+ + R_A \simeq R^+$), 4–2 ($R^- + R_A \simeq R^-$) and 1–2 (R_{2W}) using a four channel 500 MHz bandwidth oscilloscope. Current through the circuit was determined from the voltage drop in a well-calibrated ohmic resistance (R_p). Two pulsing protocols were used: 1 kHz 10 V square pulses of 30 μs width were applied to measure the dependence of the two terminal resistance (R_{2W}) with the number of pulses N, and a 1 ms width triangular ±10 V waveform was used in order to obtain the I–V characteristics of each interface. As a consequence of the use of R_p in series with the interface resistances, the effective voltage drop in each contact was reduced to ~±1.5 V, with currents ranging up to ~45 mA. Similar results were obtained for a time width in the 100 μs to 10 ms range. All the experiments were performed at room temperature. The temperature remains constant within ±0.2 K and was monitored using a Pt thermometer placed in good thermal contact with the sample. Lower pulsing frequencies were avoided as overheating effects can be observed.

3. Results and discussion

By accumulating a convenient series of pulses of the same polarity, the high resistance state of R^+ can be shifted from ~40 to ~1000 Ω and then recovered by applying pulses of inverted polarity [8]. The resistance R^- evolves in a complementary manner, i.e. when R^+ increases, R^- decreases. Here, we would like to consider the initial configuration of having R^+ in the high resistance state while R^- is in the low, in order to prepare the state needed for a resistive switching upon applying positive pulses of voltage V higher than a threshold temperature dependent value V_c [15]. By applying the first pulsing protocol, the evolution of the instant resistance of the two electrodes in series (R_{2W}) as a function of an increasing number of pulses N can be observed in figure 2. It should be noted that the main contribution to the resistance switching comes from the most resistive electrode (in this particular case from $R^+ \sim 900\,\Omega$), as most of the electric field drops in that particular interface as a consequence of the fact that the resistance of the bulk sample is negligible and that the R^- value is low (~20–30 Ω).

During the first $N \sim 40$ pulses, R_{2W} follows a noisy trend to diminish its value, and then, a sudden change is observed, followed by a nearly constant evolution, which indicates the switching to a lower and more stable non-volatile value. It is interesting to note that the noisy behaviour indicates that the changes produced in the overall resistance of R_{2W} are not always to lower values. This characteristic is probably associated with the fact that the non-volatile change in resistance observed in the RS effect is related to the electric field-induced growth of different conducting phases within the oxide interface, as a consequence of the migration of oxygen (or vacancies) [16], which generate a conduction scenario dominated by the physics of percolation. In this sense, not only is the relative proportion of the conducting phase important but also its spatial distribution, particularly if the induced-migration forms correlated structures.

At this point, the idea is to illustrate the dynamical change of the interface resistance observed for each pulse in figure 2 and the very moment when it is produced. Starting again from a configuration where R^+ is in the high state (in this case ~45 Ω, after different series of pulse treatments) while R^- is in the low (~28 Ω), I–V characteristics of each contact were obtained by applying the second pulsing protocol, where $N = 10$ repeated cycles were completed. The instant resistance of each contact was then calculated as the corresponding ratio $R^{(+,-)} = V^{(+,-)}/I$.

The results are shown in figure 3, where the evolution of the resistance of each contact can be seen as the number of cumulated cycles N is increased (inset). A gradual reduction in the R^+ value is clearly observed with each cycle while

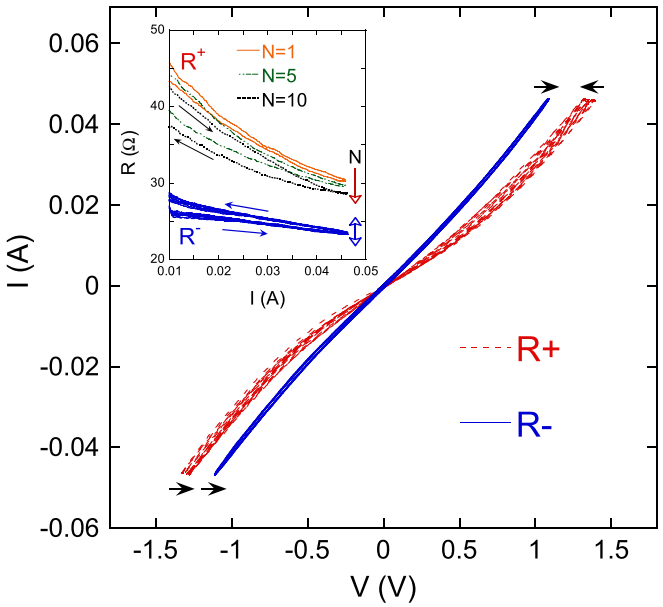

Figure 3. Ten successive voltage cycles ($N = 1 - 10$) showing the evolution of the I–V characteristics of contacts R^+ and R^-. The arrows indicate the overall evolution for each semi-cycle: R^- shows a bipolar dependence while R^+, independently of the sign of the pulse, evolves to lower values. The inset shows the current dependence of R^+ and R^- for each positive semi-cycle. For clarity, only cycles $N = 1$, 5, 10 are shown for R^+. The vertical arrows indicate the evolution of the curves with the increasing number of cycles.

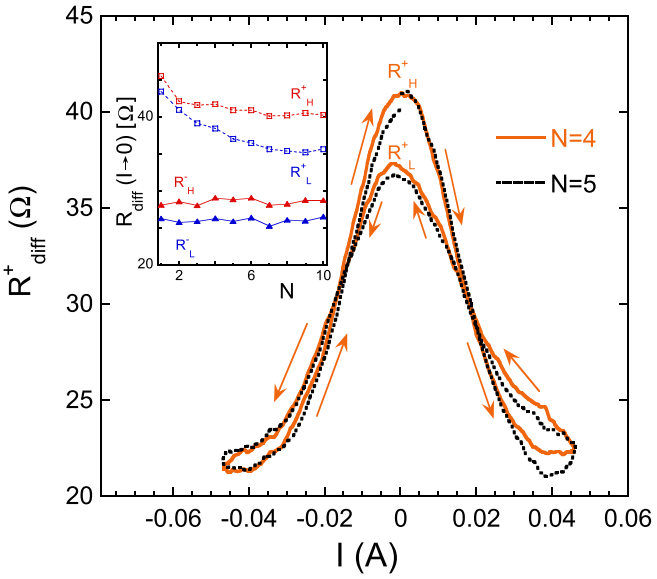

Figure 4. Differential resistance of the + contact, $R^+_{\rm diff}$, as a function of the applied current. Two typical cycles are shown ($N = 4$ and $N = 5$). The arrows indicate the path followed by $R^+_{\rm diff}$ during the current cycles. The inset shows the overall evolution with the number of pulsing cycles N of $R^+_{\rm diff}$ and $R^-_{\rm diff}$ at $I \simeq 0$, i.e. the remanent resistance of each electrode. $R^+_{\rm diff}$ and $R^-_{\rm diff}$ show bipolar behaviour. While the former varies between two well-defined states, the latter evolves asymptotically to lower values.

R^- remains nearly constant, although two different non-linear paths are reproduced in each cycle. Again, it should be noted that most of the electric field applied to electrodes 1–2 is dropping in R^+. Although both contacts present essentially bipolar and complementary behaviour [15] (R^- increases in the positive semi-cycle while it decreases in the negative, and vice versa for R^+), R^+ evolves non-symmetrically to lower values, probably as a consequence of its initial out of equilibrium state.

Considering that the high-resistance state of the contact interface is related to an out-of-equilibrium distribution of oxygen vacancies [16], independently of the bipolar switching behaviour, the application of electric pulses favours the evolution to an equilibrium distribution of vacancies. This is also documented in figure 4 where the evolution of the differential resistance $R^+_{\rm diff} = {\rm d}V_{1-3}/{\rm d}I$ during the first complete cycle shows bipolar behaviour, i.e. $R^+_{\rm diff}$ switches from high to low in the first positive semi-cycle ($N = 4$), while it switches from low to high during the negative branch, but has a different path for the second cycle ($N = 4$) and a reduction of the low value for small currents (where $R^+_{\rm diff}$ coincides with the remanent value of R^+). The overall evolution of both differential resistances in their high and low states as a function of the number of cycles can be observed in the inset of figure 4.

As shown in figure 5, the dependence with current of the differential resistance of both high and low resistance states can be very well reproduced considering the simple electronic circuit shown in figure 6. The contact between the metal and the oxide produces a non-linear conducting zone, represented

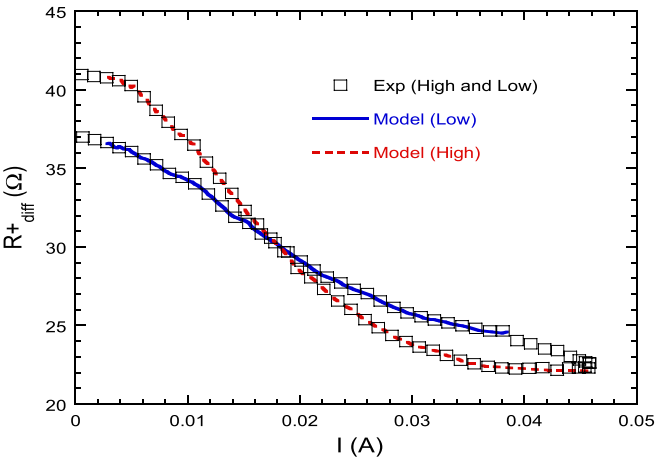

Figure 5. Differential resistance of the + contact ($R^+_{\rm diff}$) in one typical positive semi-cycle. Non-linear behaviour is observed up to the maximum applied current. When the current is reduced from its maximum value, $R^+_{\rm diff}$ switches from high to low. The high and the low resistance states are fitted following the procedure described in the text. The fitting parameters are shown in table 1.

by a diode in parallel with a resistance ($R_{\rm i}$) and both in series with the bulk resistance ($R_{\rm b}$). Two diodes in opposite direction are considered to account for the symmetry of the results with both polarities. The fits showed in figure 5 were obtained by initially solving numerically equation (1), derived from the equivalent circuit shown in figure 6 and specialized on the data of one typical positive cycle of the experimental I–V curves presented in figure 3, and then by calculating the differential

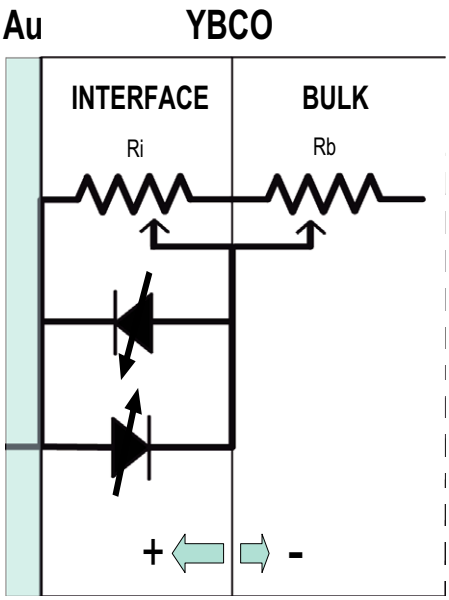

Figure 6. Schematic representation of the contact interface. A simple equivalent circuit model is also shown, which captures the dynamical evolution of R^{+}_{diff} with the applied current. When R^{+}_{diff} switches from high to low, R_{i} is reduced while R_{b} and the saturation current of the diode increase. Diodes are then represented as variable diodes. Changes are partially reversed with the negative polarity.

Table 1. Set of parameters used to fit the current dependence of the high and low states of the differential resistance R^{+}_{diff} shown in figure 5.

State	R_{i} (Ω)	R_{b} (Ω)	I_{s} (μA)
High	21	20	1
Low	14	21	8

resistance from the fitting data:

$$I = \frac{1}{1 + R_{\mathrm{b}}/R_{\mathrm{i}}} \left\{ 2I_{\mathrm{s}} \sinh\left[\frac{(V - IR_{\mathrm{b}})}{V_{\mathrm{T}}}\right] + \frac{V}{R_{\mathrm{i}}} \right\}, \qquad (1)$$

where I_{s} is the reverse bias saturation current of the diode and V_T the thermal voltage ($\simeq$26 mV at 300 K).

Practically the whole current dependence of the high and low states of R^{+}_{diff} can be fitted with a set of constant parameters, shown in table 1. The importance of this fact is that it fixes the very moment when the switching occurs: in a small current cycle part just after its reduction from the maximum attained value, and not when the critical I_{c} value is reached, as it is usually observed for binary oxide interfaces [7, 17]. This switching dynamics was observed for all the I–V cycles analyzed, indicating the generality of the effect, probably associated with the particular oxygen mobility and its influence on the electrical properties of the perovskite oxides [18].

The switching from the high to the low state produces a decrease in R_{i}, a small increase in R_{b} and a metallization of the diode, evidenced by an increase in I_{s}, naturally indicating that the interface zone is becoming more conducting. This behaviour can be expected from an electric field-induced increase in the oxygen content of the interface, in accordance with the model described by Rozenberg *et al* [16].

4. Conclusions

I–V characteristics of metal–YBCO interfaces are measured and a simple circuit model with diodes and resistances is determined, which reproduces very well the non-linear current dependence of the differential resistance. The variation of the fitting parameters when a resistance switch from a high to a low resistance state is produced is consistent with an electric field-induced metallization of the interface zone. The presented results reveal that the RS that produces the non-volatile change of the remanent resistance occurs in a particular current region. More experimental studies are needed to gain insight into this feature, probably associated with a particular oxygen (or vacancy) dynamics and its influence on local doping.

Acknowledgments

The author would like to acknowledge the financial support by CONICET Grant PIP 112-200801-00930, UBACyT X166 (2008-2010) and Dupont-Conicet 2010 MemoSat. The author is grateful to V Bekeris for a critical reading of the manuscript, P. Levy, M. J. Sánchez, M. J. Rozenberg and R. Weht for fruitful discussions, and D. Giménez, E. Pérez Wodtke and D. Rodríguez Melgarejo for technical assistance.

References

[1] Beck A, Bednorz J G, Ch. Gerber, Rossel C and Widmer D 2000 *Appl. Phys. Lett.* **77** 139
[2] Liu S Q, Wu N J and Ignatiev A 2000 *Appl. Phys. Lett.* **76** 2749
[3] Tulina N A, Ionov A M and Chaika A N 2001 *Physica* C **366** 23
[4] Seo S *et al* 2004 *Appl. Phys. Lett.* **85** 5655
[5] Fors R, Khartsev S I and Grishin A M 2005 *Phys. Rev.* B **71** 045305
[6] Quintero M, Levy P, Leyva A G and Rozenberg M J 2007 *Phys. Rev. Lett.* **98** 116601
[7] Sawa A 2008 *Mater. Today* **11** 28
[8] Acha C and Rozenberg M J 2009 *J. Phys.: Condens. Matter* **21** 045702
[9] Freitas R F and Wilcke W W 2008 *IBM J. Res. Dev.* **52** 439
[10] Waser R and Aono M 2007 *Nature Mater.* **6** 833
[11] Shi L, Shang D S, Sun J R and Shen B G 2009 *J. Appl. Phys.* **105** 083714
[12] Strukov D B, Snider G S, Stewart D R and Williams R S 2008 *Nature* **453** 80
[13] Jeong H Y, Lee J Y and Choi S-Y 2010 *Appl. Phys. Lett.* **97** 042109
[14] Nian Y B, Strozier J, Wu N J, Chen X and Ignatiev A 2007 *Phys. Rev. Lett.* **98** 146403
[15] Acha C 2009 *Physica* B **404** 2746
[16] Rozenberg M J, Sánchez M J, Weht R, Acha C, Gomez-Marlasca F and Levy P 2010 *Phys. Rev.* B **81** 115101
[17] Waser R, Dittmann R, Staikov G and Szot K 1995 *J. Appl. Phys.* **78** 6113
[18] Lacorre P, Goutenoire F, Bohnke O, Retoux R and Laligant Y 2000 *Nature* **404** 856